J Neurophysiol 124: 868–882, 2020.
First published August 12, 2020; doi:10.1152/jn.00739.2019.

RESEARCH ARTICLE | *Modularity and Compositionality in Motor Control: Acknowledging Emilio Bizzi*

Reorganization of motor modules for standing reactive balance recovery following pyridoxine-induced large-fiber peripheral sensory neuropathy in cats

Aiden M. Payne,[1] Andrew Sawers,[2] Jessica L. Allen,[3] Paul J. Stapley,[4] Jane M. Macpherson,[4] and Lena H. Ting[1,5]

[1]*The Wallace H. Coulter Department of Biomedical Engineering, Georgia Tech and Emory University, Atlanta, Georgia;* [2]*Department of Kinesiology and Nutrition, University of Illinois at Chicago, Chicago, Illinois;* [3]*Department of Chemical and Biomedical Engineering, West Virginia University, Morgantown, West Virginia;* [4]*Neurological Sciences Institute, Oregon Health and Science University, Beaverton, Oregon; and* [5]*Department of Rehabilitation Medicine, Division of Physical Therapy, Emory University, Atlanta, Georgia*

Submitted 6 December 2019; accepted in final form 31 July 2020

Payne AM, Sawers A, Allen JL, Stapley PJ, Macpherson JM, Ting LH. Reorganization of motor modules for standing reactive balance recovery following pyridoxine-induced large-fiber peripheral sensory neuropathy in cats. *J Neurophysiol* 124: 868–882, 2020. First published August 12, 2020; doi:10.1152/jn.00739.2019.—Task-level goals such as maintaining standing balance are achieved through coordinated muscle activity. Consistent and individualized groupings of synchronously activated muscles can be estimated from muscle recordings in terms of motor modules or muscle synergies, independent of their temporal activation. The structure of motor modules can change with motor training, neurological disorders, and rehabilitation, but the central and peripheral mechanisms underlying motor module structure remain unclear. To assess the role of peripheral somatosensory input on motor module structure, we evaluated changes in the structure of motor modules for reactive balance recovery following pyridoxine-induced large-fiber peripheral somatosensory neuropathy in previously collected data in four adult cats. Somatosensory fiber loss, quantified by postmortem histology, varied from mild to severe across cats. Reactive balance recovery was assessed using multidirectional translational support-surface perturbations over days to weeks throughout initial impairment and subsequent recovery of balance ability. Motor modules within each cat were quantified by non-negative matrix factorization and compared in structure over time. All cats exhibited changes in the structure of motor modules for reactive balance recovery after somatosensory loss, providing evidence that somatosensory inputs influence motor module structure. The impact of the somatosensory disturbance on the structure of motor modules in well-trained adult cats indicates that somatosensory mechanisms contribute to motor module structure, and therefore may contribute to some of the pathological changes in motor module structure in neurological disorders. These results further suggest that somatosensory nerves could be targeted during rehabilitation to influence pathological motor modules for rehabilitation.

NEW & NOTEWORTHY Stable motor modules for reactive balance recovery in well-trained adult cats were disrupted following pyridoxine-induced peripheral somatosensory neuropathy, suggesting somatosensory inputs contribute to motor module structure. Furthermore, the motor module structure continued to change as the animals regained the ability to maintain standing balance, but the modules generally did not recover pre-pyridoxine patterns. These results suggest changes in somatosensory input and subsequent learning may contribute to changes in motor module structure in pathological conditions.

electromyography; muscle synergies; sensory loss

INTRODUCTION

Task-level goals such as maintaining balance while standing and walking are achieved through coordinated muscle activity, which may change with training, impairment, or rehabilitation. Consistent and individualized groupings of synchronously activated muscles can be estimated from muscle recordings in terms of motor modules or muscle synergies, independent of their temporal activation. Analyses of motor module structure, meaning the relative levels of activation across muscles within a module and the number of motor modules, have provided insight into mechanisms of motor impairment and recovery in neurological disorders (Ting et al. 2015). For example, fewer motor modules and the activation of a greater number of muscles within each module are associated with balance and mobility impairments in people with Parkinson's disease (Rodriguez et al. 2013), cerebral palsy (Steele et al. 2015b), spinal cord injury (Fox et al. 2013; Hayes et al. 2014), and stroke (Allen et al. 2019; Clark et al. 2010; Gizzi et al. 2011; Routson et al. 2014). Motor modules can also change with training or rehabilitation. For example, long-term ballet training sculpts locomotor modules into more precise groups of fewer muscles (Sawers et al. 2015b). Similarly, rehabilitation can remediate some of the impairments in muscle coordination in people who have had a stroke (Routson et al. 2013) or people with Parkinson's disease (Allen et al. 2017). A better understanding of the central and sensory mechanisms that contribute to the spatial organization of muscle recruitment (i.e., motor modules) could facilitate more targeted strategies to improve performance in sports or activities of daily living in people with motor impairments.

Correspondence: L. H. Ting (lting@emory.edu).

A variety of studies have suggested neurons in the central nervous system structure the grouping of muscles into motor modules. The brain stem and spinal cord are particularly implicated by the preservation of motor modules after separation from higher brain areas (Desrochers et al. 2019; Roh et al. 2011), but not after spinal cord injury (Chvatal et al. 2013). Invasive activation of spinal cord interneuronal sites in frogs by microstimulation (Bizzi et al. 1991; Loeb et al. 1993) or *N*-methyl-D-aspartate (NMDA) iontophoresis (Saltiel et al. 2001, 2005) results in modular motor outputs spanning the range of natural behaviors, providing further evidence of spinally encoded motor modules. Modules activated by spinal stimulation (Loeb et al. 1993) and most modules for frog locomotion (Cheung et al. 2005) are unchanged by surgically removing sensory inputs by cutting dorsal roots, further supporting a central rather than sensory basis of motor module structure. Additionally, although reactive recovery of standing balance in response to a sudden mechanical disturbance is initially driven by somatosensory feedback (Lockhart and Ting 2007), changing somatosensory feedback by varying the initial stance posture does not alter the motor modules for reactive balance recovery in cats (Torres-Oviedo et al. 2006) or humans (Torres-Oviedo and Ting 2010), suggesting that somatosensory feedback may contribute only to the temporal activation of motor modules, while central mechanisms constrain their structure. Furthermore, motor modules for reactive balance recovery in humans are also used for locomotion (Chvatal and Ting 2012) and anticipatory postural adjustments (Chvatal et al. 2011), suggesting that motor modules are centrally coordinated and thereby available for activation by volitional feedforward mechanisms as well as by somatosensory feedback.

However, sensory mechanisms may still contribute to motor module structure to some extent. Activation of somatosensory afferents results in coordinated activation of multiple muscles within (Laporte and Lloyd 1952) and across (Eccles and Lundberg 1958) joints due to divergent synaptic connections in heterogenic reflex circuits (Eccles et al. 1957; Lundberg 1979). Although reactive balance recovery occurs at a longer latency than heterogenic reflexes and relies on the integration of visual, vestibular, and somatosensory inputs (Allum et al. 1998; Joseph Jilk et al. 2014; Peterka 2002), the initial balance-correcting muscle activity depends largely on somatosensory feedback, as evidenced by delays after somatosensory loss (Stapley et al. 2002) but not after removal of vestibular or visual inputs (Inglis and Macpherson 1995). Although motor modules for reactive balance recovery are robust to changes in initial stance posture (Torres-Oviedo et al. 2006; Torres-Oviedo and Ting 2010), stance postures have a limited range, and the associated changes in somatosensory feedback are further limited by biomechanical constraints (Burkholder and van Antwerp 2013; Steele et al. 2015a), which prevent independent stretching of muscles that cross the same joint (Kutch and Valero-Cuevas 2012). In contrast, motor modules activated by spinal microstimulation in cats are modified by large changes in limb position, suggesting an influence of position-dependent somatosensory feedback in motor module structure (Lemay and Grill 2004). Additionally, although locomotor modules tend to be similar in the partial (Santuz et al. 2019) or complete (Markin et al. 2012) absence of somatosensory feedback, this is only true for a limited subset of locomotor behaviors (Santuz et al. 2019) and when only single-joint muscles are being considered (Markin et al. 2012).

Pyridoxine toxicity selectively damages large-diameter peripheral sensory neurons and has been used to examine the effect of somatosensory loss on individual muscle recruitment. At low toxic levels, pyridoxine progressively destroys peripheral afferent populations in order of decreasing axon diameter (Hoover et al. 1981; Schaumburg et al. 1983; Xu et al. 1989), such that primary muscle spindles are more susceptible to damage than Golgi tendon organs, followed by secondary spindles, cutaneous afferents, etc. (Boyd and Davey 1968; Lloyd and Chang 1948; Rexed and Therman 1948). Although the exact mechanism of pyridoxine damage is unknown, pyridoxine enters the sensory afferents through the cell bodies in the dorsal root ganglia, which lie outside of the blood brain barrier, while limited active transport of pyridoxine across the blood-brain barrier protects motor neurons and other neurons in the central nervous system (Rao et al. 2014). We previously showed that pyridoxine-induced large-fiber neuropathy impairs reactive balance recovery in cats and that the cats eventually regain balance ability over a period of days or weeks without regeneration of somatosensory afferent fibers (Lockhart and Ting 2007; Stapley et al. 2002). Although motor responses to translational perturbations lose the initial burst of balance-correcting muscle activity after pyridoxine (Stapley et al. 2002), the temporal pattern of activation still follows kinematic errors for balance recovery (Lockhart and Ting 2007). Our prior reports of changes at the muscle and behavioral level did not assess changes in motor module structure, which could reveal the extent to which somatosensory feedback contributes to the coupling between muscles.

To assess whether somatosensory feedback contributes to the coupling between muscles, we assessed whether the motor modules for reactive balance recovery are affected by large-diameter peripheral neuropathy. We found that the structure of stable motor modules for reactive balance recovery in well-trained adult cats were disrupted following pyridoxine-induced peripheral somatosensory neuropathy, suggesting somatosensory inputs contribute to motor module structure.

METHODS

Ethics statement. Data for this study were collected at Oregon Health and Science University between 2000 and 2003. The original protocol was approved by the Institutional Animal Care and Use Committee of the Oregon Health and Science University and conformed to National Institutes of Health guidelines for the care and treatment of animals. Some of the animals included in this study have been included in previously published studies asking different scientific questions about pyridoxine (Lockhart and Ting 2007; Stapley et al. 2002) or assessing motor modules (Ting and Macpherson 2005; Torres-Oviedo et al. 2006) or other aspects of postural responses (Ting and Macpherson 2004) in the healthy (pre-pyridoxine) state or as control animals in the healthy (pre-pyridoxine) state for comparison against cats with vestibular loss (Macpherson et al. 2007; Stapley et al. 2006).

Overview. To assess the role of large-diameter somatosensory afferents in the coordination of muscle activity for reactive balance recovery, we applied motor module analyses to previously collected electromyography (EMG) data from cats during multidirectional postural perturbations before and after pyridoxine-induced somatosensory neuropathy (Lockhart and Ting 2007; Stapley et al. 2002). Four healthy adult female cats (ranging from 3.3 to 4.9 kg) were trained

Table 1. *List of muscles recorded from left hindlimb of all cats in proximal to distal order by joint crossings*

Muscle	Label	Cat			
		Br	Kn	St	Sq
Adductor femoris magnus	ADFM	X		X	X
Gluteus medius	GLUT		X		
Iliopsoas	ILPS		X		
Biceps femoris anterior	BFMA	X		X	X
Biceps femoris medialis	BFMM	X	X	X	X
Biceps femoris posterior	BFMP	X			X
Gracilis	GRAC	X			X
Rectus femoris	REFM	X	X	X	X
Semimembranosus anterior	SEMA	X	X	X	
Semimembranosus posterior	SEMP	X	X	X	X
Sartorius anterior	SRTA	X	X	X	X
Semitendinosus	STEN	X	X	X	
Lateral gastrocnemius	LGAS			X	
Medial gastrocnemius	MGAS	X			X
Plantaris	PLAN			X	X
Vastus lateralis	VLAT		X		
Vastus medialis	VMED	X		X	X
Peroneus brevis	PERB	X		X	X
Soleus	SOL		X		
Tibialis anterior	TIBA		X	X	X
Extensor digitorum longus	EDL	X		X	X
Flexor digitorum longus	FDL	X		X	X
Flexor hallucis longus	FHL	X		X	X

with positive reinforcement to stand quietly on four force plates mounted on a moving platform (Coulmance et al. 1979; Macpherson et al. 1987). Once trained, 11 (n = 1 animal) or 16 (n = 3 animals) muscles of the left hindlimb (Table 1) were implanted with chronic indwelling EMG electrodes in each cat (Macpherson 1988). Translational support-surface perturbations were applied in 12 evenly spaced directions in the horizontal plane during standing (Fig. 1) (Stapley et al. 2002). Somatosensory neuropathy was elicited by intraperitoneal injections of pyridoxine (Stapley et al. 2002), and the extent of neuropathy was quantified in postmortem histology. Data collection resumed on *day 1* or *2* following initial injection and continued over a series of days until the animals were euthanized (Table 2). Motor modules were extracted using nonnegative matrix factorization (NMF) (Chvatal and Ting 2012; Lee and Seung 1999; Torres-Oviedo and Ting 2007) and compared before and after sensory loss to assess the role of large-diameter peripheral afferents in the coordination of muscle activity for reactive balance recovery.

Pyridoxine administration. Low toxic doses of pyridoxine were administered to elicit large-fiber somatosensory neuropathy without damaging motor neurons. After baseline data collection, cats were injected intraperitoneally with pyridoxine in the late afternoon according to the schedule in Table 2, using a range of dosages to induce varied degrees of somatosensory neuropathy. Three of the four cats received a second dose of pyridoxine the day after the first dose (Table 2).

Histology. Anatomical loss of large-diameter afferent fibers was quantified in postmortem histology in the four pyridoxine cats and compared against that in five control cats used in other postural studies. Cat Kn was euthanized on *day 15* (after pyridoxine injection), and the remaining three cats were euthanized at a later time (Table 2). At the longer survival times, degeneration was complete and cellular debris had cleared allowing easier analysis of nerve tissues. Each cat was deeply anesthetized and perfused intracardially to harvest cutaneous and mixed peripheral nerves as described in Stapley et al. (2002). MetaMorph image analysis system (Universal Imaging, West Chester, PA) was used to quantify the cross-sectional area of all myelinated fibers, estimating fiber diameters assuming a circular cross section.

We report data from distal saphenous (all cats) and zygomaticotemporal (cat Br only) cutaneous nerves and lateral triceps brachii (all cats) and medial gastrocnemius (cat Br only) mixed nerves. The distal saphenous nerve and the medial gastrocnemius nerves were sampled 20 mm and 10 mm proximal to the ankle joint, respectively. The zygomaticotemporal nerve was sampled just past the branch point off from the trigeminal nerve. The lateral triceps brachii nerve was sampled as far as possible from the entry point into the muscle because the fiber diameters become smaller as the fibers branch near the muscle (Eccles and Sherrington 1930).

Histograms of the diameters of all the normal fibers (myelin + axon) larger than 1 μm were created using a bin width of 0.5 μm, with cumulative sum plots overlaid. Histograms and cumulative sum plots for the control animals include means and SD across the control animals. The extent of neuropathy was determined by comparing histograms and cumulative sums between pyridoxine cats and the control data for each nerve (Fig. 2). The diameter at which each pyridoxine cat's fiber count fell 1 SD below the mean of the control cats was chosen as the cutoff value where significant neuropathy began. Although fiber loss occurred within the range of motor neuron diameters, i.e., α-motoneurons 9–17 μm; γ-motoneurons 2–8 μm (Boyd and Davey 1968; Rexed and Therman 1948), motor neurons are protected from pyridoxine damage by the blood-brain barrier (Rao et al. 2014). To remove variation of the cumulative sum plots due to variability in the smaller diameter fibers, we chose to begin the

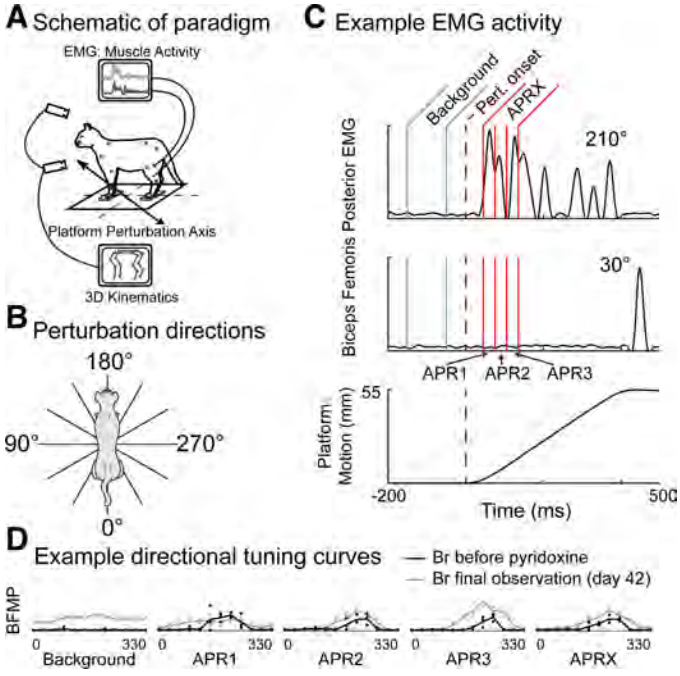

Fig. 1. Balance-correcting motor responses were elicited by multidirectional translational perturbations. *A*: schematic of perturbation paradigm. Implanted electromyography (EMG) electrodes were used to record muscle activity from muscles of the left hindlimb in response to translational perturbations. *B*: perturbations were given in 12 equally spaced directions in the horizontal plane. *C*: example EMG activity from biceps femoris posterior in perturbation directions 210° and 30° from cat Br. The onset of platform motion is indicated by a vertical dashed line. Gray lines indicate the background time bin (50–150 ms before perturbation onset). Red lines indicate the 3 consecutive 30-ms time bins of the active response (APR1, APR2, APR3), beginning at the onset of the balance-correcting response visually identified for each cat before pyridoxine administration. The APRX time bin contains the 3 active time bins. *D*: example directional tuning curves show the activation of the biceps femoris posterior muscle (BFMP) in cat Br across perturbation directions for each time bin before pyridoxine (black) and on the final day of observation (*day 42*; gray) for comparison. 3D, 3-dimensional; Pert., perturbation.

Table 2. *Pyridoxine dosing and testing schedule for each animal*

Cat	*Day 0:* First Dose, mg/kg	*Day 1*: Second Dose, mg/kg	Days Tested	Day of Euthanasia
Br	350	260	***−1***, ***1***, *2*, *11*, *18*, *21*, *23*, ***24***, ***39***, ***42***	*43*
Kn	350	350	***−73***, ***−45***, ***1***, ***2***, ***3***, ***4***, *5*, *6*, *7*, ***8***	*15*
St	350	0	***−46***, *1*, *2*, *3*, *7*, *8*, ***15***, ***16***	*36*
Sq	350	175	***−32***, ***1***, ***2***, ***3***, ***4***, ***5***, ***6***, ***18***	*31*

Days tested are in bold for days in which enough trials were collected for motor module analysis.

cumulative sum plots for the mixed nerves at the 6-μm bin for cats Sq, St, and Kn, making the cutoff for fiber loss more clear.

Tendon tap reflexes. Tendon tap reflex amplitudes were quantified in a single muscle attached to the Achilles tendon as a simple indicator of low-level functional impairment. Tendon tap reflexes were assessed in medial gastrocnemius (MGAS) for Br and Sq, lateral gastrocnemius (LGAS) for St, and soleus (SOL) for Kn as described by Stapley et al. (2002). One experimenter held the cat upright in the air without explicit control of initial muscle length while another experimenter administered the tendon taps using an instrumented piece of Plexiglas shaped to cup the Achilles tendon. Up to 10 trials of 40 taps to the Achilles tendon were recorded during control sessions and on various days after pyridoxine. EMG data and tap pulses during tendon tap trials were sampled at 3,000 Hz, high-pass filtered at 35 Hz (3rd-order zero-lag Butterworth filter), mean-subtracted, rectified, and low-pass filtered at 35 Hz using custom MATLAB routines. Tendon tap reflexes were quantified as the difference in EMG amplitude between the pre-tap baseline (mean EMG 35–50 ms before tap stimulus) and the peak amplitude of the EMG response in the first 15 ms after the tap stimulus. Tendon tap reflex amplitudes were compared across days within cats using a two-way ANOVA ($\alpha = 0.05$). We report the day at which a sustained reduction in the tendon tap reflex amplitude begins relative to pre-pyridoxine based on post hoc Tukey tests ($\alpha = 0.05$).

Perturbations. Postural responses were elicited by sudden translations of the support surface before pyridoxine and on a series of days after pyridoxine depending on the ability of each cat (Table 2). When weight distribution was approximately even between left and right sides during standing, translational perturbations of the support surface were applied in 12 evenly spaced directions in the horizontal plane (ramp and hold, 55-mm amplitude; 15 cm/s mean peak velocity) (Fig. 1) (Stapley et al. 2002). Up to five trials were recorded for each perturbation direction on each day of testing, with a written record indicating whether the cat was balanced at the end of the trial, meaning the cat did not step or fall over, and whether the cat received external support from an experimenter during the trial. Only the trials in which the cats maintained balance without external support were considered for analysis. To prevent biases in the motor module analysis due to differences in the number of trials across directions and days, only the first three balanced and unsupported trials in each perturbation direction were included in the motor module analysis for each day. Days with less than three balanced trials in any perturbation direction were excluded from analysis, with the exception of cat Kn, who had perturbation direction 240 excluded from analysis on all days due to the inability to balance in this perturbation direction on the final day (*day 8*).

Muscle activity in perturbations. EMG (1,000 Hz) data collection began 300 ms before platform displacement, collecting a total of 3 s for each perturbation trial. EMG data were high-pass filtered at 35 Hz (3rd-order zero-lag Butterworth filter), mean-subtracted, rectified, and low-pass filtered at 35 Hz offline using custom MATLAB routines. This filtering results in an envelope of the rectified EMG signal (Fig. 1*C*).

EMG activity was then quantified as the mean activity level in four time bins, consisting of a background time bin 50–150 ms before perturbation and three consecutive 30-ms active time bins (APR1, APR2, APR3; Fig. 1) beginning at the onset of the balance-correcting response visually identified for each cat before pyridoxine. APR1 began at 45 ms for Br, 50 ms for Sq, and 55 ms for Kn and St. The choice not to shift the time bins with previously described delays in the motor response after pyridoxine (Stapley et al. 2002) was made to prevent capturing a larger portion of subsequent voluntary behaviors at later time points and to avoid issues identifying muscle onset latencies at later time points with large-amplitude background EMG activity and the lack of a clear transition to the active response. Additionally, we have since clarified that although the initial motor response is reduced by pyridoxine, the onsets often become shallower in slope rather than delayed in latency (Lockhart and Ting 2007), which is more apparent when activity is compared across perturbation directions.

Directional tuning curves display the binned muscle or module activation magnitudes as a function of perturbation direction (Macpherson 1988; Ting and Macpherson 2005). In the case of the motor modules, these tuning curves relate to the function of generating end-point forces in certain directions (Ting and Macpherson 2005; Torres-Oviedo et al. 2006), while the muscle tuning curves are more variable due to membership in multiple modules. For plotting, EMG amplitudes for each muscle in each cat were normalized to have a maximum amplitude of 1 across all time bins and trials before pyridoxine administration, and this same normalization factor was maintained across all later time points (i.e., amplitudes larger than 1 may be observed on later days for muscles that were more active after pyridoxine administration). This normalization is only for plotting and has no impact on motor module quantification, which uses a different normalization, described below. Figure 1*D* shows example tuning curves for each time bin in a single muscle as an example (more examples in Supplemental Fig. S1; all Supplemental material can be found at https://github.com/AidenPayne/B6-Cat-Supplemental; https://doi.org/10.5281/zenodo.3922881). For compactness in figures, the activity across the three active time bins is further averaged into a combined APRX time bin for plotting, which is shown instead of the three active time bins in subsequent figures. Note that with the exception of cat Br (Fig. 1*D*), we observed directionally tuned motor responses in APR1 in most muscles after pyridoxine, indicating that the active response still begins in APR1 in most cases.

Motor module structure. Motor module analysis was applied separately to the binned matrices of postural EMG activity from each day of testing in each cat as previously described (Chvatal and Ting 2012; Torres-Oviedo and Ting 2007). To ensure that each muscle was equally weighted in the motor module analysis, each row of the EMG data matrix (i.e., the activity within each muscle within each day of testing across all time bins and trials) was renormalized to have unit variance during module extraction (Torres-Oviedo and Ting 2007). Nonnegative matrix factorization (NMF) (Lee and Seung 1999) was then applied to factor each input data matrix into a matrix of module weights (spatial structure) and another matrix of activation coefficients (directional tuning curves), which can be multiplied together to reconstruct (an approximation of) the input data matrix of muscle activity. The NMF algorithm was separately applied to extract each possible number of motor modules from each data matrix, with a minimum of one module and a maximum number of modules equal to

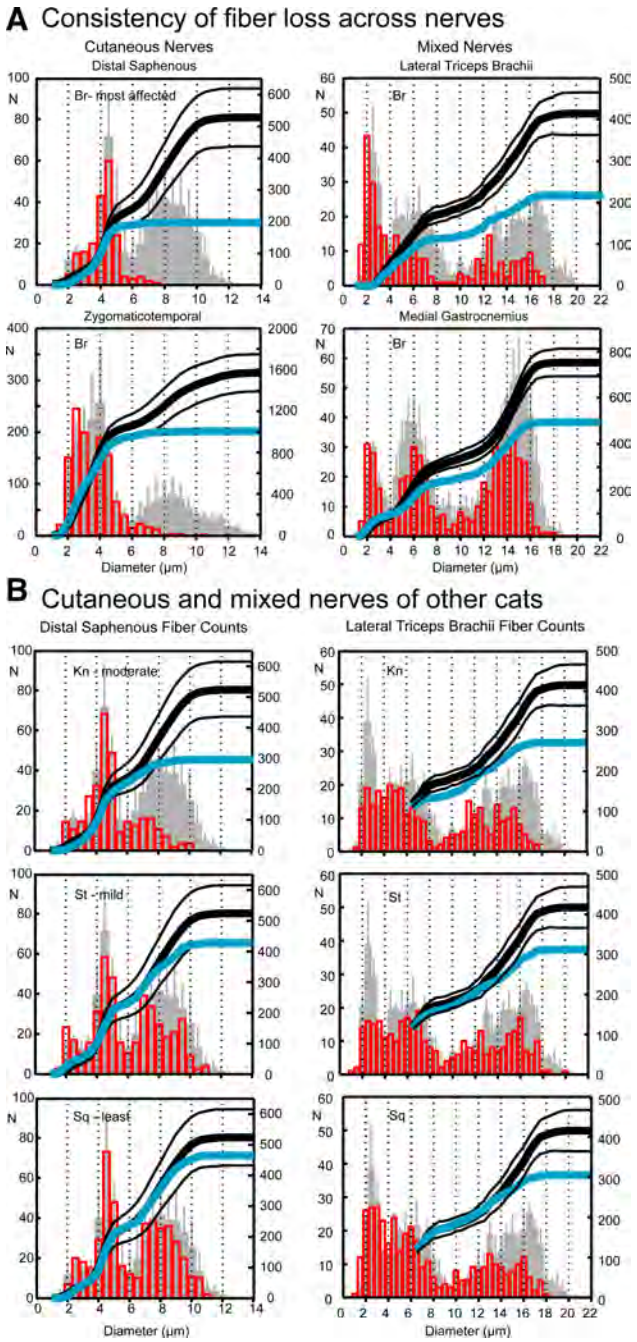

Fig. 2. Histology. *A*: fiber loss was consistent across nerves. Red histograms show fiber counts (*N*) by afferent diameter in the most severely affected cat (Br). Gray histograms show the mean and SD of fiber counts for 5 control cats used for other studies. Blue lines show cumulative fiber counts for cat Br. Black lines indicate the mean and SD of cumulative counts for the control cats. Cat Br showed significant loss of axons >4–5 μm in diameter in cutaneous and mixed nerves of the hindlimb (distal saphenous, medial gastrocnemius), forelimb (lateral triceps brachii), and head (zygomaticotemporal). *B*: the diameter above which significant loss occurred varied across cats. Cat Kn was moderately affected, with significant loss of fibers above 6–7 μm in diameter. Cats St and Sq were mildly affected, with significant loss of fibers above 12–13 μm and 14–15 μm in diameter, respectively.

the number of muscles recorded in each animal (i.e., a maximum of 11 modules for Kn or 16 otherwise).

The EMG data matrices were then reconstructed using the extracted motor modules, and the goodness of fit of data reconstruction was quantified for each number of motor modules based on the variance accounted for (VAF), which measures the fraction of variability in the data set that can be accounted for by the extracted vector modules (Torres-Oviedo and Ting 2007; Zar 1999). That is, the VAF quantifies how well the muscle activity (i.e., the directional tuning curves input into the motor module analysis) can be reconstructed as a linear combination of the motor module weight matrices according to the module directional tuning curves (which are also an output from the motor module analysis). The 95% confidence intervals on the VAF were calculated by a bootstrapping procedure where the EMG data sets were resampled 500 times with replacement and the VAF of the reconstructed EMG was recalculated after each resampling (Sawers et al. 2015b). The number of motor modules to report for each data set was selected as the smallest set of motor modules for which the lower bound of the 95% confidence interval exceeded 90% VAF in data reconstruction (Cheung et al. 2005; Hayes et al. 2014). Changes in complexity of the motor responses were assessed by changes in the number of motor modules between initial and final observations using a paired two-way *t* test ($\alpha = 0.05$).

Modularity was compared with chance levels determined from shuffled EMG data matrices. Because NMF will factor any data set into vector modules regardless of whether or not an underlying structure is present, we compared the VAF for each possible number of modules in each data set with the VAF similarly obtained from a shuffled version of the same data set, where correlations between muscles were removed by randomly reordering the activity within each muscle (i.e., independently shuffling the data points within each row or muscle of the data matrix across trials and time bins). Separation between the upper bound of the confidence intervals for the VAF of the shuffled EMG data matrix and the lower bound of the confidence intervals for the VAF of the original EMG data matrix indicates that the original EMG data matrix contains more structure or modularity (i.e., the muscles are more coordinated or more correlated) than would be expected by chance.

Changes in motor modules were assessed by the reduction in VAF when motor modules were used to reconstruct EMG data from subsequent days (Fig. 3). Across cats, a paired *t* test was used to compare the VAF when pre-pyridoxine modules were used to reconstruct the pre-pyridoxine data compared with the VAF when data were reconstructed from the final day to test for changes in motor module structure at the group level ($\alpha = 0.05$). Additionally, within cats, nonoverlapping confidence intervals on the VAF when the same modules were used to reconstruct data from subsequent days indicate a significant change in the motor modules across days.

Changes in motor modules within cats were additionally assessed by comparing similar motor modules between initial and final observations. Unit variance scaling during module extraction was reverted before plotting module structure and comparing structure of modules across days. Changes in motor module structure were quantified by using Pearson's correlation coefficient (*r*) to compare the structure of motor modules before pyridoxine with the structure of motor modules on subsequent days. For modules with 16 muscles (cats Br, St, and Sq), a significant change in module structure is defined as $r < 0.497$, corresponding to the critical *r* value for $\alpha = 0.05$ (for $n = 16$ muscles, $n - 2 = 14$ degrees of freedom). For modules with 11 muscles (cat Kn), a significant change in module structure is defined as $r < 0.602$ for $\alpha = 0.05$ (for $n = 11$ muscles, $n - 2 = 9$ degrees of freedom). A pair of motor modules are considered similar across days when the *r* value for their comparison is above the critical *r* value. Because it is unclear whether a pair of similar modules observed on different days represent a single module that has changed over time or the use of distinct modules that appear similar, this does not present a strict measure of changes in motor modules but allows for a more qualitative comparison of modules across days. While it is possible that changes in EMG signal quality over time impacted motor module structure, the comparison of two pre-pyridoxine time points separated by nearly a month in cat Kn (see Fig. 6) suggests such an effect is

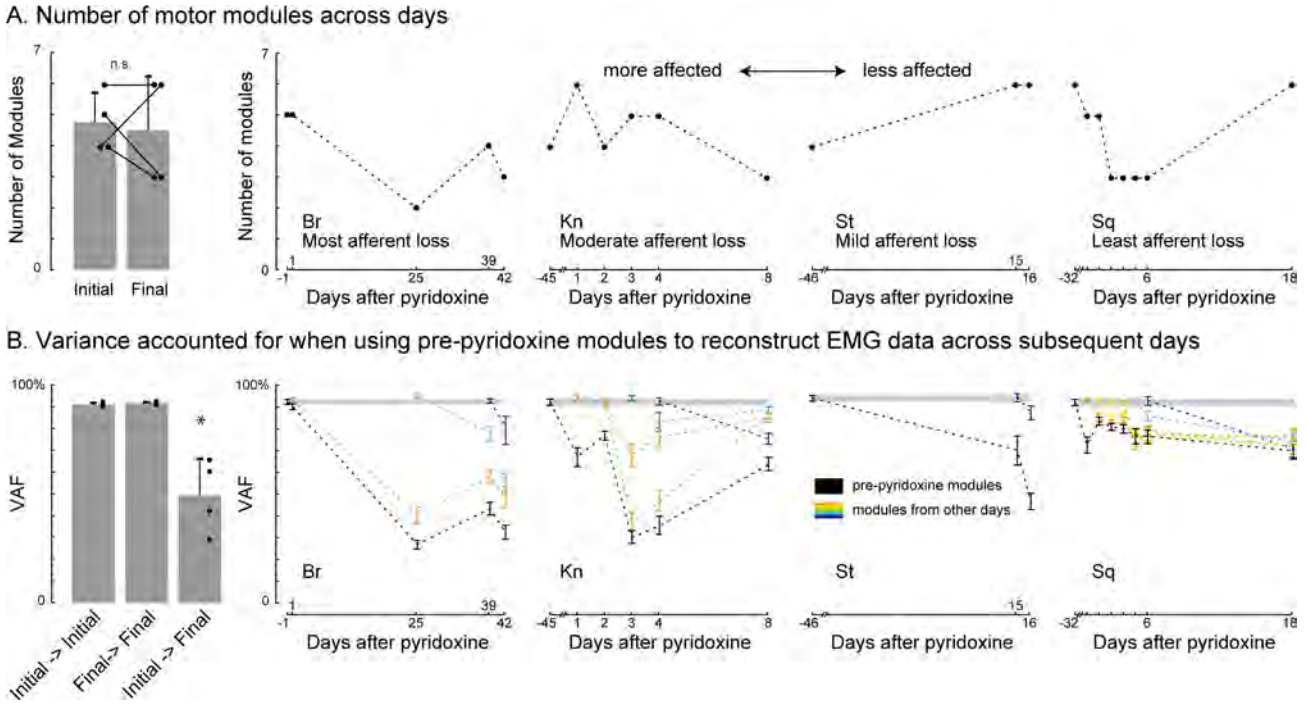

Fig. 3. Changes in motor modules were not consistent across cats. *A*: bar plot shows no significant group-level change in the number of motor modules between initial and final days. Line plots show the number of modules over time within each animal, ordered from most severe afferent loss (Br; >4–5 μm) on the *left* to least afferent loss (Sq; >15–16 μm) on the *right*. *B*: bar plot shows a significant group-level reduction in variance accounted for (VAF) when pre-pyridoxine modules were applied to reconstruct electromyography (EMG) data from the final day. Line plots show the 95% confidence intervals for the VAF when the pre-pyridoxine motor modules (black) were applied to reconstruct EMG data on all subsequent days within each cat. Other colors show 95% confidence intervals for the VAF when modules from intermediate days were applied to reconstruct EMG data across subsequent days.

small if present. Multiple pre-pyridoxine time points are not available for the other cats.

In modules that were similar in structure, changes in directional tuning were also quantified using Pearson's correlation coefficient (r) to compare directional tuning curves in each of the active time bins (APR1, APR2, APR3) between pre-pyridoxine and later days. Changes in directional tuning were similarly quantified in the combined active time bin (APRX). When tuning curves with 12 data points for each of the 12 perturbation directions (cats Br, St, and Sq) were compared, a significant change in directional tuning was defined as $r < 0.576$ for $\alpha = 0.05$ (for $n = 12$ directions, $n - 2 = 10$ degrees of freedom). When tuning curves with 11 data points in cat Kn were compared, a significant change in directional tuning was defined as $r < 0.602$ for $\alpha = 0.05$ (for $n = 11$ directions, $n - 2 = 9$ degrees of freedom). A pair of directional tuning curves are considered similar across days when the r value for their comparison is above the critical r value.

RESULTS

Effects of pyridoxine on nerve loss, stretch reflexes, and balance behavior. All cats showed a loss of axons above a certain diameter within the range of afferent fiber diameter sizes (Table 3). The diameter above which fiber loss occurred differed between cats but was consistent within cats across nerves (Fig. 2). Cat Br was profoundly affected with loss of all group I and II afferents as inferred from the fiber diameter profiles. Figure 2*A* illustrates the consistency of fiber loss in Br across cutaneous and mixed nerves of the hindlimb, forelimb, and head. Cat Kn was moderately affected as evident in cutaneous and mixed nerve profiles (Fig. 2*B*). Cats St and Sq were least affected, with little or no involvement of cutaneous nerves, which did not exceed 12–14 μm in diameter in the control cats. Fiber loss of the larger afferents was evident in the mixed nerves of these cats (medial gastrocnemius and lateral triceps brachii, Fig. 2*B*).

All cats showed a sustained reduction in tendon tap reflex amplitude after pyridoxine, although the time at which this occurred varied across cats. A reduction in the tendon tap response amplitude was observed and sustained after *day 5* in cat Br ($P < 0.0001$), *day 7* in cat Kn ($P < 0.0001$), and *day 1* in cat St ($P < 0.0001$) and cat Sq ($P < 0.0001$).

Cats displayed balance impairments ranging from those that did not limit the ability to stand or walk (i.e., minor) to those that resulted in the inability to walk or crawl for weeks (i.e., severe). The most severely affected cat (Br; loss of afferents >5–6 μm in diameter) was severely ataxic by *day 3* and

Table 3. *Fiber diameters above which fiber loss was observed for each cat and types of afferents inferred to remain intact*

Cat	Fiber Diameter, μm	Afferent Species Assumed to Remain Intact
Br	5–6	Group III – slow cutaneous, down hair receptors
Kn	7–8	Small proportion of cutaneous and spindle 2°
St	13–14	Most cutaneous and spindle 2°; small proportion of spindle 1°, GTOs
Sq	15–16	All spindle 2°, cutaneous; majority of spindle 1°, GTOs

GTOs, Golgi tendon organs. Data for afferent species are from Boyd and Davey (1968), Lloyd and McIntyre (1948), and Rexed and Therman (1948).

unable to stand without assistance from *day 2* to *day 21*, but maintained balance independently from *day 23* onward. The moderately affected cat (Kn; loss of afferents >7–8 μm in diameter) was very ataxic by *day 4* and unable to stand without assistance from *day 5* to *day 7*, but maintained balance in most perturbation directions on *day 8* (Stapley et al. 2002). A mildly affected cat (St; loss of afferents >13–14 μm in diameter) maintained balance without assistance on all days at which a full translation run was completed but fatigued too rapidly to complete a full run between *day 2* and *day 15*. The least affected cat (Sq; loss of afferents >15–16 μm in diameter) maintained balance without assistance at all time points.

Group-level changes in motor modules after pyridoxine. EMG activity was well described by a modular spatial structure at initial and final observations, but the structure of the individual modules differed across observations. In all cats, a modular low-dimensional structure of the EMG data is apparent in the separation between the 95% confidence intervals on the VAF for the selected number of modules between real and shuffled data sets at both initial and final observations (see Figs. 4, 5, 7, and 8). In each cat, changes in motor module structure between the initial and final observations were demonstrated by a decrease in VAF when the original motor modules were used to reconstruct EMG data on the final vs. the initial observation (Fig. 3*B*; $P = 0.020$). Reconstructions at the final observations ranged from 32% in the most affected cat (Br) to 70% in the least affected cat (Sq). In contrast, use of cat Kn's original modules to reconstruct another time point before pyridoxine injection yielded 86% VAF (using modules from 45 days before pyridoxine to reconstruct EMG from 73 days before pyridoxine).

There were no significant group-level changes in the number of motor modules between initial and final time points (Fig. 3*A*; $P = 0.79$). However, the number of motor modules was not constant across days within the individual cats. The more impaired cats showed reductions in the number of motor modules, from five to three in severely affected cat Br and from four to three in moderately affected cat Kn. In contrast, the less affected cats maintained (6 modules in mildly affected cat Sq) or increased the number of motor modules (from 4 to 6 in mildly affected cat St) between initial and final observations.

Case series study within each animal. While the group-level changes demonstrate that motor modules changed in structure after pyridoxine, the specific changes cannot be easily summarized at the group level due to differences in the muscles observed, the extent of sensory loss, and the time course of behavioral recovery. For this reason, we present a more in-depth description of each cat as a case series below, in order of descending severity of afferent fiber loss, so that changes in motor modules may be considered in relation to the extent of sensory loss, behavioral impairments, and time course of behavioral recovery specific to each cat.

Br: most severely affected animal. Motor responses to perturbations in the most severely affected cat continued to be modular after pyridoxine, but the modules varied in structure over time. The separation of the VAF between real and shuffled data sets narrowed, particularly on *day 25* (Fig. 4), but the confidence intervals did not overlap on any of the days tested, indicating a persisting modular structure of the motor responses. Five motor modules exceeded 90% VAF in the motor responses before pyridoxine. These same motor modules yielded significantly lower VAF when data were reconstructed from subsequent days (Fig. 3*B*; nonoverlapping confidence intervals, means range 25–40%), indicating a change in the motor modules after pyridoxine. On the final day (*day 42*), only three motor modules were needed to exceed 90% VAF in data reconstruction.

Each of the motor modules observed on the final day (*day 42*) was comparable in both structure and directional tuning to one of the pre-pyridoxine motor modules (Fig. 4). The module that was most similar in structure (Fig. 4, *bottom*, orange module, second row; $r = 0.848$) was also the most similar in directional tuning ($r = 0.855$) in the combined APRX time bin and did not differ in directional tuning in any of the APR time bins (APR1, $r = 0.629$; APR2, $r = 0.845$; APR3, $r = 0.794$). The second most conserved module in structure (Fig. 4, *bottom*, light green module, third row; $r = 0.811$) was similar in directional tuning in APR1 ($r = 0.905$) and APR2 ($r = 0.680$) but not in APR3 ($r = 0.103$), indicating that changes in activation were not always most prominent in APR1. The least conserved module in structure (Fig. 4, *bottom*, red module, first row; $r = 0.599$) was similar in directional tuning in APR2 ($r = 0.817$) and APR3 ($r = 0.897$) but not APR1 ($r = 0.112$).

Kn: moderately affected animal. Motor responses to perturbations in the moderately affected cat continued to be modular after pyridoxine, but the modules varied in structure over time. The separation of the VAF between real and shuffled data sets narrowed, particularly on the first day after pyridoxine (Fig. 5), but the confidence intervals did not overlap, indicating a persisting modular structure of the motor responses. Four motor modules exceeded 90% VAF in the motor responses before pyridoxine. These same motor modules yielded significantly lower VAF when data were reconstructed from all subsequent days (Fig. 3*B*; nonoverlapping confidence intervals, means range 32–77%), with the lowest VAF of 30% on *day 3* and a VAF of 63% on the final day (*day 8*), indicating a change in the motor modules after pyridoxine. On the final day (*day 8*), only three motor modules were needed to exceed 90% VAF in data reconstruction.

The three motor modules observed on the final day (*day 8*) had limited overlap in structure or directional tuning to the pre-pyridoxine motor modules. One of the final motor modules was similar in structure (Fig. 6, light green module, third row; $r = 0.768$) but not directional tuning ($r = 0.230$) to one of the original modules, appearing to lack directional tuning at all on the final day (*day 8*). Another module was similar in directional tuning (Fig. 6, light blue module, fourth row; $r = 0.793$) but not structure ($r = 0.546$) to one of the original modules. Although this module (Fig. 6, light blue module, fourth row) was not similar in structure between initial and final days, it is aligned and compared based on similarity to modules on intermediate days. The third module observed on the final day (Fig. 5, *bottom*, and Fig. 6, dark green module, fifth row) was not similar to any of the pre-pyridoxine modules in structure or directional tuning. In contrast, all four of the pre-pyridoxine motor modules (*day −45*) were similar in structure to the modules from another pre-pyridoxine day of testing (*day −73*) that were nearly a month apart (Fig. 6).

St: Mildly affected animal. Motor responses to perturbations in the mildly affected cat continued to be modular after pyridoxine, but the modules varied in structure over time. The confidence intervals on the VAF between real and shuffled data

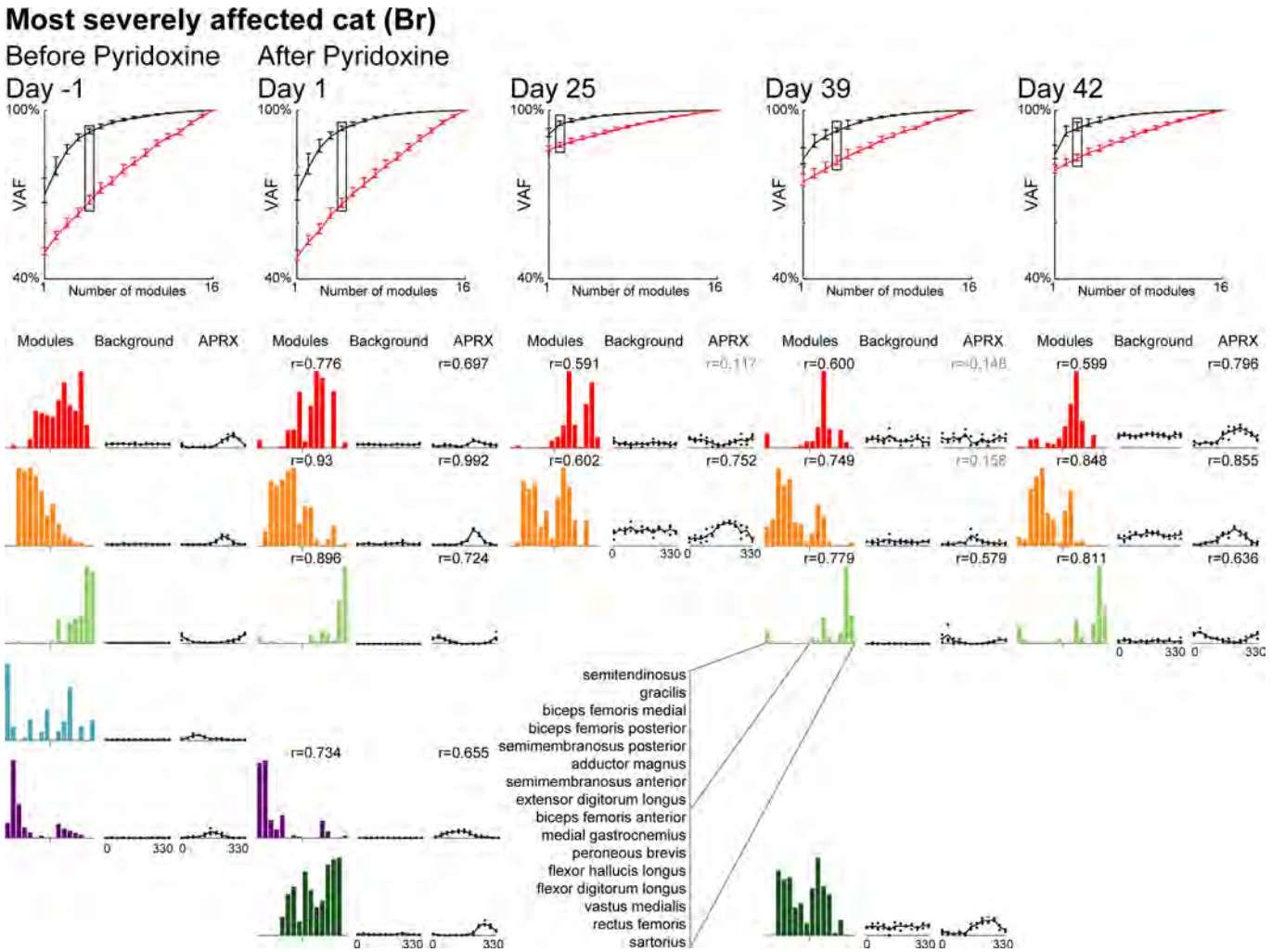

Fig. 4. Motor modules for the most severely affected cat (Br). *Top*: plots show the variance accounted for (VAF) by each possible number of motor modules for the electromyography (EMG) data in black and a shuffled version of the EMG data in red. Boxes are drawn to indicate the selected number of motor modules for the data on each day, based on the criterion that the lower bound of the 95% confidence interval exceeds 90% VAF. *Bottom*: motor modules for each day of testing. The spatial structure (weight matrices) of motor modules is shown as bar plots that are aligned across days based on similarity (quantified by Pearson's *r*, relative to pre-pyridoxine). A significant change in motor module structure is indicated by $r < 0.497$ for $\alpha = 0.05$ (for $n = 16$ muscles, $n - 2 = 14$ degrees of freedom). The directional tuning curves show the activation of each motor module as a function of perturbation direction in the pre-perturbation background time bin and the combined active (APRX) time bin. Similarity of directional tuning curves in the APRX time bin is also quantified by Pearson's *r* relative to pre-pyridoxine. A significant change in directional tuning is indicated by $r < 0.576$ for $\alpha = 0.05$ (for $n = 12$ directions, $n - 2 = 10$ degrees of freedom).

sets did not overlap on any day of testing, indicating a persisting modular structure of the motor responses (Fig. 7). Four motor modules exceeded 90% VAF in the motor responses before pyridoxine. Use of these same modules to reconstruct data from subsequent days yielded significantly lower VAF (Fig. 3*B*; nonoverlapping confidence intervals), with 63% VAF on *day 15* and 42% VAF on the final day (*day 16*), indicating a change in the motor modules after pyridoxine. On the final day (*day 16*), six modules were needed to exceed 90% VAF in data reconstruction.

Three of the six motor modules observed on the final day (*day 16*) were comparable in structure to one of the pre-pyridoxine motor modules. The module that was the most conserved in structure (Fig. 7, *bottom*, light green module, third row; $r = 0.829$) between initial and final observations was also the most conserved in directional tuning ($r = 0.956$). The next most conserved module in structure (Fig. 7, *bottom*, red module, first row; $r = 0.776$), was not similar in directional tuning ($r = 0.572$), although directional tuning of this module is not apparent on any day. The other module that was conserved in structure (Fig. 7, *bottom*, orange module, second row; $r = 0.625$) was also similar in directional tuning ($r = 0.883$). The remaining three modules were not similar to any of the pre-pyridoxine modules.

Sq: Least affected animal. Motor responses to perturbations in the least affected cat continued to be modular after pyridoxine, but the modules varied in structure over time. The separation of the VAF between real and shuffled data sets narrowed, particularly on *day 6* (Fig. 8), but the confidence intervals did not overlap, indicating a persisting modular structure of the motor responses. Six motor modules exceeded 90% VAF in the motor responses before pyridoxine. Use of the pre-pyridoxine modules to reconstruct the data on subsequent days yielded significantly lower VAF on all subsequent days (Fig. 3*B*; nonoverlapping confidence intervals, means range 70–83%), accounting for 70% VAF on the final day (*day 18*),

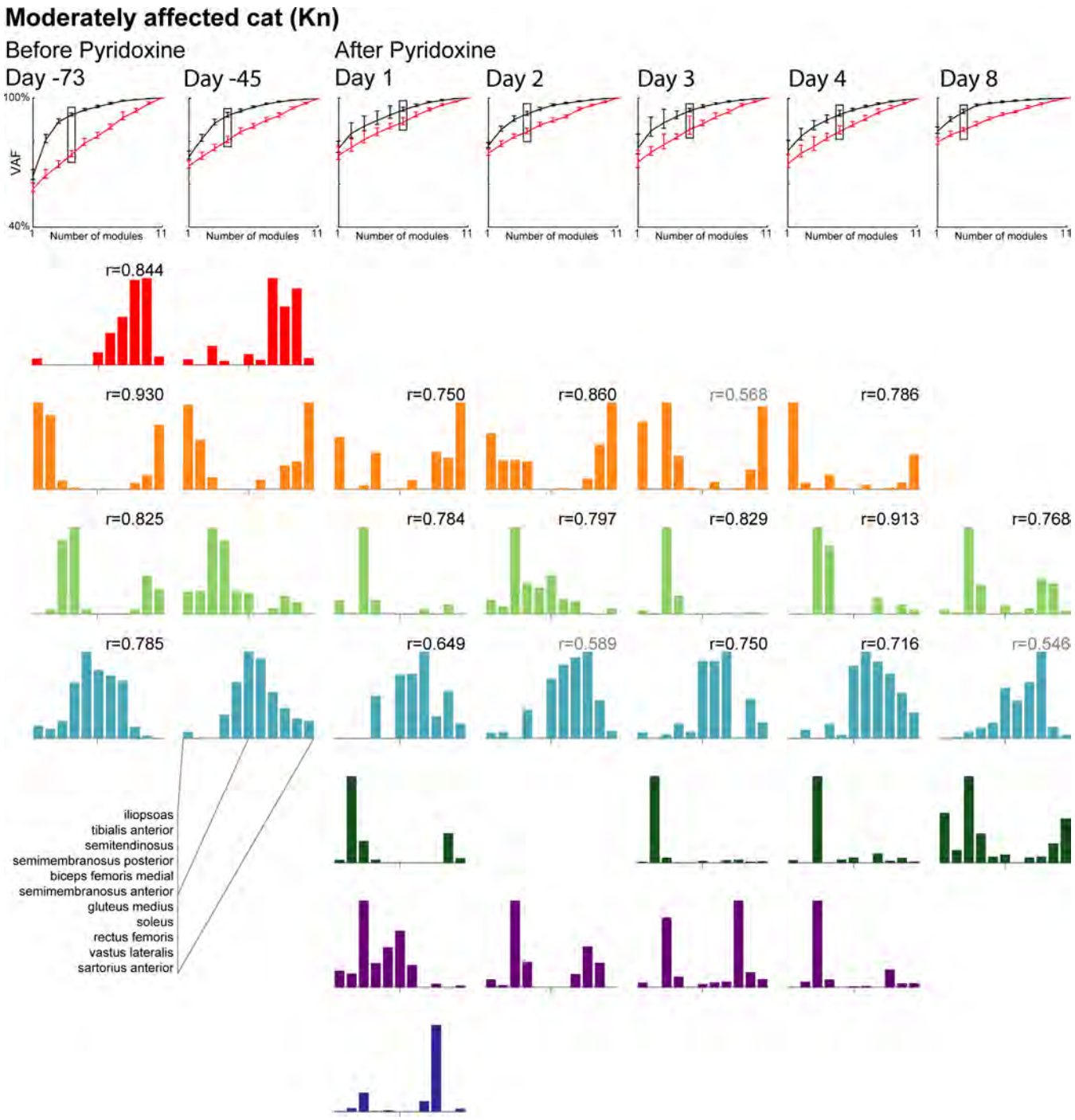

Fig. 5. Motor modules for the moderately affected cat (Kn). *Top*: plots show the variance accounted for (VAF) by each possible number of motor modules for the electromyography (EMG) data in black and a shuffled version of the EMG data in red. Boxes are drawn to indicate the selected number of motor modules for the data on each day, based on the criterion that the lower bound of the 95% confidence interval exceeds 90% VAF. *Bottom*: motor modules for each day of testing. The spatial structure (weight matrices) of motor modules is shown as bar plots that are aligned across days based on similarity (quantified by Pearson's *r*, relative to pre-pyridoxine *day −45*). A significant change in motor module structure is indicated by $r < 0.602$ for $\alpha = 0.05$ (for $n = 11$ muscles, $n - 2 = 9$ degrees of freedom). Note that the light blue module (fourth row) is aligned across days despite significant differences in module structure based on similarity of directional tuning.

indicating that the motor modules in cat Sq changed to a lesser extent than those in the more affected cats after pyridoxine. On the final day (*day 18*), six motor modules were again required to exceed 90% VAF in data reconstruction, with four of these modules comparable to original modules in both structure and directional tuning (Fig. 8).

DISCUSSION

Stable motor modules for reactive balance recovery were disrupted in well-trained adult cats by a partial loss of somatosensory afferents. Motor modules continued to change as the animals regained the ability to stand independently. Pyridoxine-induced peripheral neuropathy and behavioral impairments

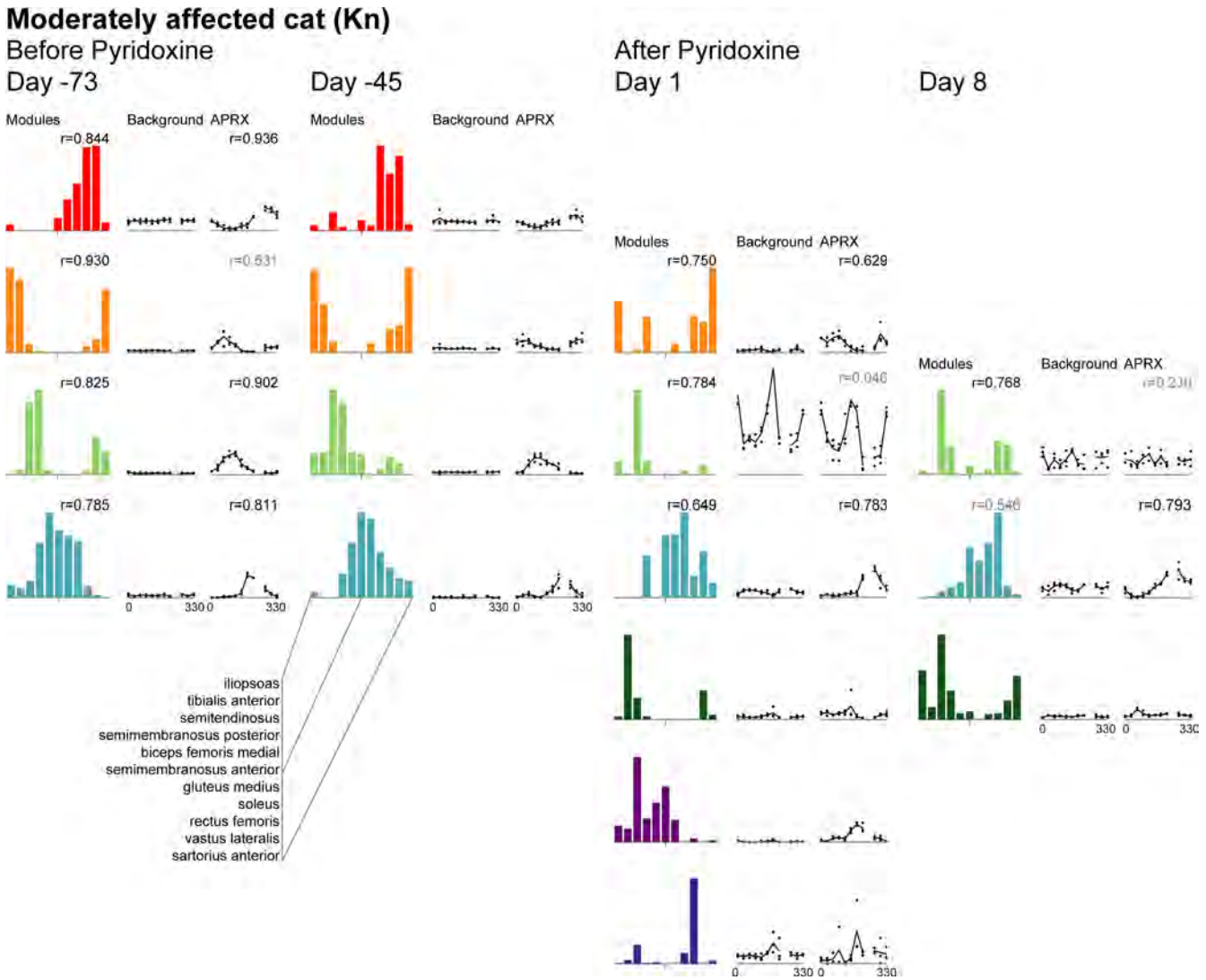

Fig. 6. Motor modules for the moderately affected cat (Kn) on select days. The spatial structure (weight matrices) of motor modules is shown as bar plots that are aligned across days based on similarity (quantified by Pearson's *r*, relative to pre-pyridoxine *day −45*). A significant change in motor module structure is indicated by $r < 0.602$ for $\alpha = 0.05$ (for $n = 11$ muscles, $n - 2 = 9$ degrees of freedom). The directional tuning curves show the activation of each motor module as a function of perturbation direction in the pre-perturbation background time bin and the combined active (APRX) time bin. Similarity of directional tuning curves in the APRX time bin are also quantified by Pearson's *r* relative to pre-pyridoxine. A significant change in directional tuning is indicated by $r < 0.602$ for $\alpha = 0.05$ (for $n = 11$ directions, $n - 2 = 9$ degrees of freedom). Note that the light blue module (fourth row) is aligned across days despite significant differences in module structure to enable comparison of directional tuning.

varied in severity across cats. All cats exhibited changes in motor modules over days to weeks after pyridoxine that were much greater than typical changes between sessions (Torres-Oviedo et al. 2006; Torres-Oviedo and Ting 2010), suggesting a role for somatosensory feedback in the structure of motor modules for reactive balance recovery. The initial changes in motor module structure likely resulted from direct effects of pyridoxine damage to somatosensory neurons, followed by compensatory changes in the more impaired cats. We observed gradual changes in some modules, while others disappeared or appeared between sessions. Despite limitations of small sample size and differences in available data across cats, we provide evidence that a disruption in somatosensory information can drive rapid day-to-day changes in motor modules for well-learned reactive balance recovery behavior in adult cats. Given that this somatosensory impairment impacted motor module structure, rather than only changing temporal activation of preexisting modules, some of the pathological changes in motor module structure in clinical populations could similarly arise from somatosensory impairments. Along these same lines, the impact of somatosensory inputs on motor module structure suggests it may be possible to target somatosensory nerves to influence pathological motor modules for rehabilitation.

Pyridoxine resulted in a range of behavioral impairments corresponding to the severity of afferent fiber loss. Consistent with another group that used pyridoxine to elicit afferent fiber loss in cats, we did not observe a dose-dependent relationship between pyridoxine and the extent of afferent fiber loss (Allum et al. 1998), but the extent of afferent fiber loss was related to behavioral impairments. Based on the diameter of fibers that were damaged, we surmise that the least affected cat lost only a subset of the primary muscle spindle afferents, which did not impair balance ability. Damage to primary muscle spindle

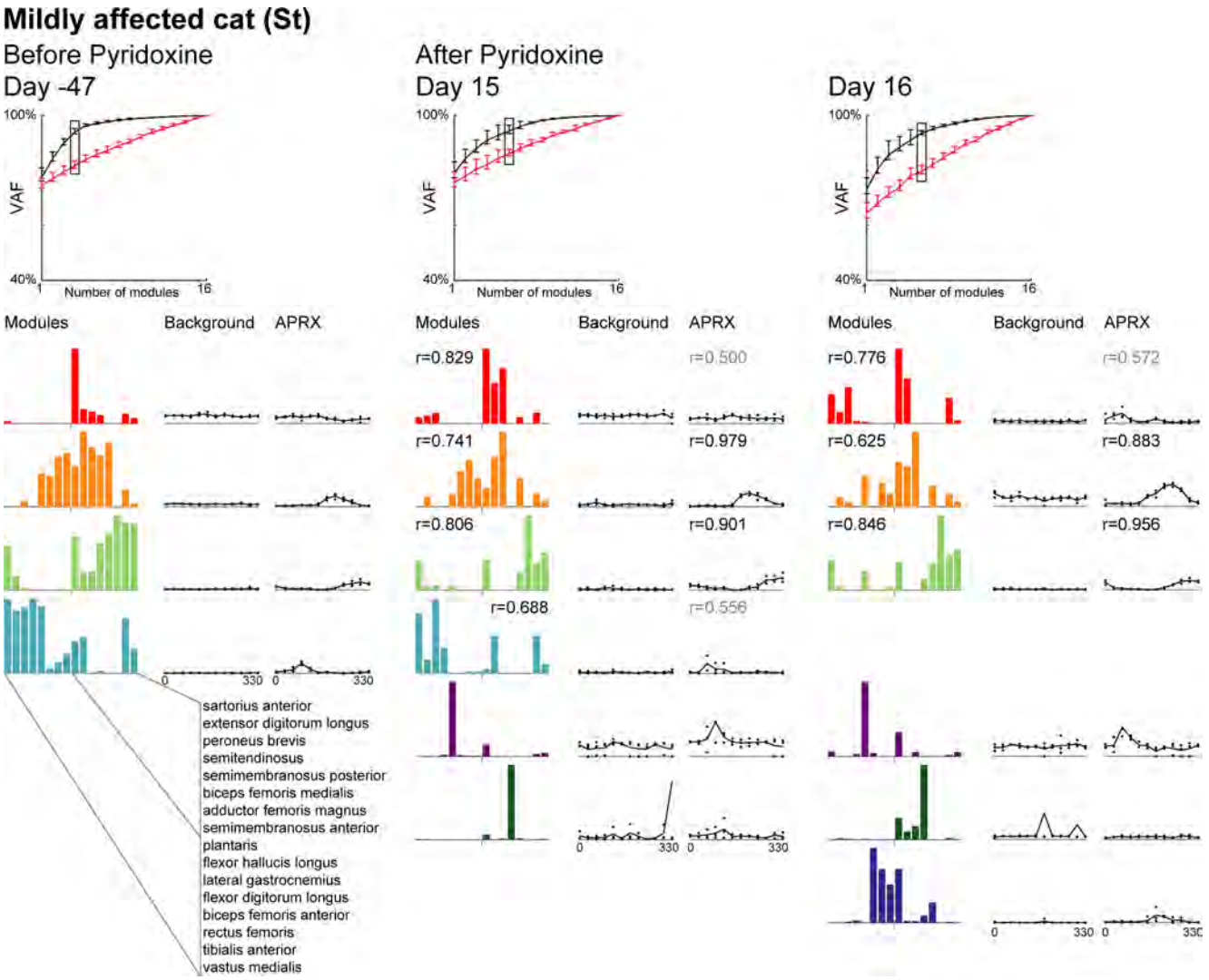

Fig. 7. Motor modules for the mildly affected cat (St). *Top*: plots show the variance accounted for (VAF) by each possible number of motor modules for the electromyography (EMG) data in black and a shuffled version of the EMG data in red. Boxes are drawn to indicate the selected number of motor modules for the data on each day, based on the criterion that the lower bound of the 95% confidence interval exceeds 90% VAF. *Bottom*: motor modules for each day of testing. The spatial structure (weight matrices) of motor modules is shown as bar plots that are aligned across days based on similarity (quantified by Pearson's *r*, relative to pre-pyridoxine). A significant change in motor module structure is indicated by $r < 0.497$ for $\alpha = 0.05$ (for $n = 16$ muscles, $n - 2 = 14$ degrees of freedom). The directional tuning curves show the activation of each motor module as a function of perturbation direction in the pre-perturbation background time bin and the combined active (APRX) time bin. Similarity of directional tuning curves in the APRX time bin is also quantified by Pearson's *r* relative to pre-pyridoxine. A significant change in directional tuning is indicated by $r < 0.576$ for $\alpha = 0.05$ (for $n = 12$ directions, $n - 2 = 10$ degrees of freedom).

afferents is additionally supported by the impacted tendon tap responses in all cats. Lack of balance impairment in the least affected cat is consistent with the lack of impairment in postural sway of humans with Charcot-Marie-Tooth type IA, whose fiber loss is restricted to group I afferents (Nardone et al. 2000). In contrast, the most severely affected cat may have lost the majority of afferents from primary and secondary muscle spindles, Golgi tendon organs, and receptors for touch, and was unable to walk or crawl for weeks after pyridoxine administration. The severe balance impairment in the most affected cat is consistent with human studies showing severe balance impairments in human patients with severe loss of leg proprioception caused by dorsal root ganglionopathy (Dalakas 1986; Griffin et al. 1990).

Motor module structure changed in all cats, suggesting somatosensory inputs influence the structure of motor modules for reactive balance recovery. We previously showed motor modules for balance recovery are stable over days of testing (Torres-Oviedo et al. 2006; Torres-Oviedo and Ting 2010), and here we show the modules are stable over a month between sessions before pyridoxine in one of our cats (Kn; Fig. 6, first 2 columns of modules). In contrast, module structure changed in all of the cats in the days to weeks following pyridoxine, demonstrating that a change in somatosensory inputs can destabilize the structure of motor modules for reactive balance recovery. While changes in the number of motor modules were not consistent across cats, no cat maintained the same number of modules across all days, indicating the use of different modules on different days. The declining VAF when using modules to reconstruct EMG data across subsequent days indicates a progressive change in motor module structure over time. Interestingly, in the moderately impaired cat Kn, the pre-pyridoxine modules were better able to reconstruct data from the final day (*day 8*) than some of the intermediate days

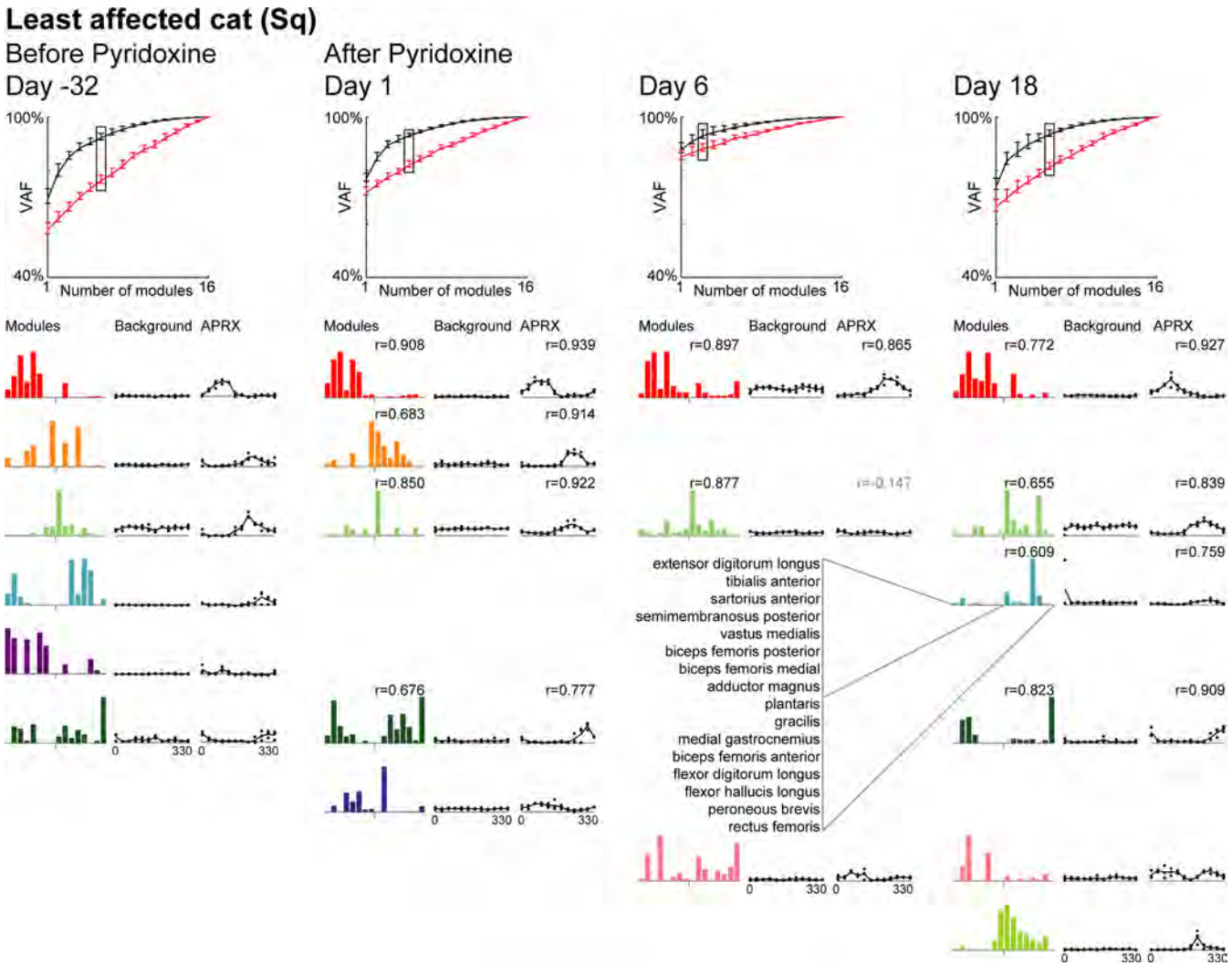

Fig. 8. Motor modules for the least affected cat (Sq) on select days. *Top*: plots show the variance accounted for (VAF) by each possible number of motor modules for the electromyography (EMG) data in black and a shuffled version of the EMG data in red. Boxes are drawn to indicate the selected number of motor modules for the data on each day, based on the criterion that the lower bound of the 95% confidence interval exceeds 90% VAF. *Bottom*: motor modules for select days of testing. The spatial structure (weight matrices) of motor modules is shown as bar plots that are aligned across days based on similarity (quantified by Pearson's *r*, relative to pre-pyridoxine). A significant change in motor module structure is indicated by $r < 0.497$ for $\alpha = 0.05$ (for $n = 16$ muscles, $n - 2 = 14$ degrees of freedom). The directional tuning curves show the activation of each motor module as a function of perturbation direction in the pre-perturbation background time bin and the combined active (APRX) time bin. Similarity of directional tuning curves in the APRX time bin is also quantified by Pearson's *r* relative to pre-pyridoxine. A significant change in directional tuning is indicated by $r < 0.576$ for $\alpha = 0.05$ (for $n = 12$ directions, $n - 2 = 10$ degrees of freedom).

(particularly *day 3*; Fig. 3*B*), suggesting the modules were tending back toward the pre-pyridoxine structure to some extent. Although changes in limb posture do not change motor module structure (Torres-Oviedo et al. 2006), our finding that changes in somatosensory input can change motor module structure is consistent with the changes in the structure of spinally evoked motor modules with much larger changes in limb posture (Lemay and Grill 2004).

Our results are in contrast with the persistence of most motor modules for frog locomotion following unilateral deafferentation (Cheung et al. 2005), which may be explained by differences in both the behavioral tasks and species. Frog locomotion is a feedforward behavior, which may explain the lack of changes in both behavior and motor module structure after deafferentation. In contrast, cats rely heavily on somatosensory feedback for standing balance, as demonstrated by changes in both behavior and motor module structure. Importantly, changes in motor module structure were observed in the least affected cat in the absence of behavioral impairment, indicating a direct effect of somatosensory inputs on the structure of motor modules for reactive balance recovery in the absence of compensatory learning.

We cannot differentiate between the direct effects of pyridoxine damage and the indirect effects of compensation on motor module structure. We observed some modules changing progressively across days (e.g., Fig. 5, second to fourth rows), while others disappeared or appeared across days (e.g., Fig. 5, first row and fifth to seventh rows). The progressive loss of afferent populations may explain some of the progressive changes in module structure, particularly those occurring before behavioral impairments. The loss of afferent populations may also explain some of the disappearing modules, which may have required specific afferent inputs for activation. However, similar changes in module structure may have occurred

through compensatory learning, particularly in the more impaired cats. Motor learning can cause similar changes in motor modules; for example, when rats learn to perform a novel reach-to-grasp task (Kargo and Nitz 2003), some rats progressively alter module structures alongside progressive improvements in task performance, while other rats explore the selection of different modules across trials through trial-and-error learning. While the inability to distinguish between direct and indirect effects of pyridoxine on motor module structure represents a limitation of this study, it is clear that pyridoxine damage to somatosensory neurons initiated changes in previously stable motor modules for a well-learned behavior in adult animals.

Further, the distinction between progressively changing modules versus new or lost modules is not entirely clear. We observed a module in the moderately impaired cat (Kn; Fig. 5, light blue module, fourth row) that we would have considered different between initial and final days if we had not observed the progressive changes in structure in the days between, despite the preserved directional tuning. Further, some modules that appear similar across days may reflect combinations of muscles that are mechanically required for the task. Because the cats are able to stand unassisted on all of the days that we analyzed, there is always at least one extensor module, which can be identified by its non-zero activation during the background time bin (Ting and Macpherson 2005; Torres-Oviedo et al. 2006). Further, because the cats were able to recover balance in response to the multidirectional perturbations, the directional tuning curves of the modules span the range of perturbations, related to their function of generating end-point forces for balance recovery (Ting and Macpherson 2005; Torres-Oviedo et al. 2006). Using a hindlimb biomechanical model, we previously quantified the wide feasible ranges of individual muscle forces for generation of physiological end-point forces in certain directions, demonstrating that many muscles are optional, while others are required (Sohn et al. 2013). Muscles such as soleus and sartorius are required to generate end-point forces in certain directions and are consistently represented in modules on the final day in the cats with these muscles recorded. In contrast, extensor digitorum longus is optional, as its contributions to end-point forces can be achieved by other muscles, and is not strongly activated by any module on the final day in Br or St, and is only weakly represented in modules on the final day in Sq. It is also possible that some of the transient modules reflect merging (Clark et al. 2010) or fractionation (Cheung et al. 2012) of pairs of modules that cannot be distinguished on days when their temporal activation was similar (Steele et al. 2015a).

Although our results suggest that damage to somatosensory neurons can destabilize motor module structure for a well-learned task in adult cats, there are several limitations to consider. Because we are reanalyzing previously collected data, the experiments were not designed in consideration of the present analyses. We have presented our data as a case series because our ability to make direct comparisons across cats was limited by differences in the extent of pyridoxine damage, differences in the muscles recorded, and differences in the days on which data were collected for each cat. While variation in severity enabled us to present very severe and very mild cases of impairment, some of the differences between cases may be also due to interanimal differences. In fact, many studies have observed interindividual variability in response to peripheral nerve lesions despite more rigorous control of the location and extent of lesions and the training procedures throughout recovery (Frigon 2011). While the more impaired cats showed a reduction in the number of motor modules after pyridoxine, we would need more animals at each level of severity to test for such a relationship between the loss of afferents and the loss of modules. Additionally, although the multiple intermediate days revealed a progression of changes, the cats were able to practice standing balance during natural behaviors between successful runs, which were sometimes separated by many days, presenting opportunities for the cats to adapt and learn that we were unable to observe with our motor module analyses. However, despite these limitations, we provide evidence that changes in somatosensory feedback can result in rapid day-to-day changes in the structure of motor modules for reactive balance recovery.

Our results could be explained by changes in the function of spinal interneurons after pyridoxine. While divergent heterogenic reflex pathways are insufficient to explain the modularity of motor output, particularly for feedforward behaviors, a variety of invasive animal studies have suggested that motor modules may be encoded at a higher level, in spinal interneuronal networks (Bizzi et al. 1991; Caggiano et al. 2016; Giszter et al. 1993; Hart and Giszter 2010; Levine et al. 2014; Saltiel et al. 2001, 2005; Stein and Daniels-McQueen 2002). While we cannot be certain of the mechanisms underlying changes in motor module structure after pyridoxine, it is possible that the changes in motor modules occur through changes in spinal interneuronal networks. Because the function of spinal interneurons is heavily dependent on the combination of inputs (Jankowska 1992), a change in somatosensory inputs could change motor module structure by changing the function of spinal interneurons, regardless of whether their physical connections to other neurons changed. However, behavioral recovery in the more impaired cats likely required plastic changes throughout sensorimotor circuits for balance recovery, including plasticity of the remaining afferents (Bernard et al. 2007). In addition to plasticity related to behavioral learning, sustained deprivation of inputs can cause neurons to fire spontaneously in the absence of inputs (Fröhlich et al. 2008; Turrigiano and Nelson 2000, 2004). If motor modules are encoded in spinal interneurons, which are at the interface of sensory and motor neurons, it may not be possible to dissociate sensory and motor contributions to motor module structure. Regardless of the underlying mechanism, our results suggest that a somatosensory insult can destabilize motor modules in an adult animal, which may have implications for rehabilitation.

GRANTS

This work was supported by National Institutes of Health Grants 5T90 DA032466 and R01 HD46922.

DISCLOSURES

No conflicts of interest, financial or otherwise, are declared by the authors.

AUTHOR CONTRIBUTIONS

P.J.S., J.M.M., and L.H.T. conceived and designed research; P.J.S., L.H.T., and J.M.M. performed experiments; A.M.P. and J.M.M. analyzed data;

A.M.P., A.S., J.L.A., and L.H.T. interpreted results of experiments; A.M.P. prepared figures; A.M.P. drafted manuscript; A.M.P., A.S., J.L.A., J.M.M., and L.H.T. edited and revised manuscript; A.M.P., A.S., J.L.A., P.J.S., J.M.M., and L.H.T. approved final version of manuscript.

REFERENCES

Allen JL, Kesar TM, Ting LH. Motor module generalization across balance and walking is impaired after stroke. *J Neurophysiol* 122: 277–289, 2019. doi:10.1152/jn.00561.2018.

Allen JL, McKay JL, Sawers A, Hackney ME, Ting LH. Increased neuromuscular consistency in gait and balance after partnered, dance-based rehabilitation in Parkinson's disease. *J Neurophysiol* 118: 363–373, 2017. doi:10.1152/jn.00813.2016.

Allum JH, Bloem BR, Carpenter MG, Hulliger M, Hadders-Algra M. Proprioceptive control of posture: a review of new concepts. *Gait Posture* 8: 214–242, 1998. doi:10.1016/S0966-6362(98)00027-7.

Bernard G, Bouyer L, Provencher J, Rossignol S. Study of cutaneous reflex compensation during locomotion after nerve section in the cat. *J Neurophysiol* 97: 4173–4185, 2007. doi:10.1152/jn.00797.2006.

Bizzi E, Mussa-Ivaldi FA, Giszter S. Computations underlying the execution of movement: a biological perspective. *Science* 253: 287–291, 1991. doi:10.1126/science.1857964.

Boyd IA, Davey MR. *Composition of Peripheral Nerves*. Edinburgh, UK: E & S Livingstone Ltd, 1968, p. 57.

Burkholder TJ, van Antwerp KW. Practical limits on muscle synergy identification by non-negative matrix factorization in systems with mechanical constraints. *Med Biol Eng Comput* 51: 187–196, 2013. doi:10.1007/s11517-012-0983-8.

Caggiano V, Cheung VC, Bizzi E. An optogenetic demonstration of motor modularity in the mammalian spinal cord. *Sci Rep* 6: 35185, 2016. doi:10.1038/srep35185.

Cheung VC, d'Avella A, Tresch MC, Bizzi E. Central and sensory contributions to the activation and organization of muscle synergies during natural motor behaviors. *J Neurosci* 25: 6419–6434, 2005. doi:10.1523/JNEUROSCI.4904-04.2005.

Cheung VC, Turolla A, Agostini M, Silvoni S, Bennis C, Kasi P, Paganoni S, Bonato P, Bizzi E. Muscle synergy patterns as physiological markers of motor cortical damage. *Proc Natl Acad Sci USA* 109: 14652–14656, 2012. doi:10.1073/pnas.1212056109.

Chvatal SA, Macpherson JM, Torres-Oviedo G, Ting LH. Absence of postural muscle synergies for balance after spinal cord transection. *J Neurophysiol* 110: 1301–1310, 2013. doi:10.1152/jn.00038.2013.

Chvatal SA, Ting LH. Voluntary and reactive recruitment of locomotor muscle synergies during perturbed walking. *J Neurosci* 32: 12237–12250, 2012. doi:10.1523/JNEUROSCI.6344-11.2012.

Chvatal SA, Torres-Oviedo G, Safavynia SA, Ting LH. Common muscle synergies for control of center of mass and force in nonstepping and stepping postural behaviors. *J Neurophysiol* 106: 999–1015, 2011. doi:10.1152/jn.00549.2010.

Clark DJ, Ting LH, Zajac FE, Neptune RR, Kautz SA. Merging of healthy motor modules predicts reduced locomotor performance and muscle coordination complexity post-stroke. *J Neurophysiol* 103: 844–857, 2010. doi:10.1152/jn.00825.2009.

Coulmance M, Gahéry Y, Massion J, Swett JE. The placing reaction in the standing cat: a model for the study of posture and movement. *Exp Brain Res* 37: 265–281, 1979. doi:10.1007/BF00237713.

Dalakas MC. Chronic idiopathic ataxic neuropathy. *Ann Neurol* 19: 545–554, 1986. doi:10.1002/ana.410190605.

Desrochers E, Harnie J, Doelman A, Hurteau MF, Frigon A. Spinal control of muscle synergies for adult mammalian locomotion. *J Physiol* 597: 333–350, 2019. doi:10.1113/JP277018.

Eccles JC, Eccles RM, Lundberg A. The convergence of monosynaptic excitatory afferents on to many different species of alpha motoneurones. *J Physiol* 137: 22–50, 1957. doi:10.1113/jphysiol.1957.sp005794.

Eccles JC, Sherrington CS. Numbers and contraction values of individual motor units examined in some muscles of the limb. *Proc R Soc Lond B Biol Sci* 106: 326–357, 1930. doi:10.1098/rspb.1930.0032.

Eccles RM, Lundberg A. Integrative pattern of Ia synaptic actions on motoneurones of hip and knee muscles. *J Physiol* 144: 271–298, 1958. doi:10.1113/jphysiol.1958.sp006101.

Fox EJ, Tester NJ, Kautz SA, Howland DR, Clark DJ, Garvan C, Behrman AL. Modular control of varied locomotor tasks in children with incomplete spinal cord injuries. *J Neurophysiol* 110: 1415–1425, 2013. doi:10.1152/jn.00676.2012.

Frigon A. Chapter 7–Interindividual variability and its implications for locomotor adaptation following peripheral nerve and/or spinal cord injury. *Prog Brain Res* 188: 101–118, 2011. doi:10.1016/B978-0-444-53825-3.00012-7.

Fröhlich F, Bazhenov M, Sejnowski TJ. Pathological effect of homeostatic synaptic scaling on network dynamics in diseases of the cortex. *J Neurosci* 28: 1709–1720, 2008. doi:10.1523/JNEUROSCI.4263-07.2008.

Giszter SF, Mussa-Ivaldi FA, Bizzi E. Convergent force fields organized in the frog's spinal cord. *J Neurosci* 13: 467–491, 1993. doi:10.1523/JNEUROSCI.13-02-00467.1993.

Gizzi L, Nielsen JF, Felici F, Ivanenko YP, Farina D. Impulses of activation but not motor modules are preserved in the locomotion of subacute stroke patients. *J Neurophysiol* 106: 202–210, 2011. doi:10.1152/jn.00727.2010.

Griffin JW, Cornblath DR, Alexander E, Campbell J, Low PA, Bird S, Feldman EL. Ataxic sensory neuropathy and dorsal root ganglionitis associated with Sjögren's syndrome. *Ann Neurol* 27: 304–315, 1990. doi:10.1002/ana.410270313.

Hart CB, Giszter SF. A neural basis for motor primitives in the spinal cord. *J Neurosci* 30: 1322–1336, 2010. doi:10.1523/JNEUROSCI.5894-08.2010.

Hayes HB, Chvatal SA, French MA, Ting LH, Trumbower RD. Neuromuscular constraints on muscle coordination during overground walking in persons with chronic incomplete spinal cord injury. *Clin Neurophysiol* 125: 2024–2035, 2014. doi:10.1016/j.clinph.2014.02.001.

Hoover DM, Carlton WW, Henrikson CK. Ultrastructural lesions of pyridoxine toxicity in beagle dogs. *Vet Pathol* 18: 769–777, 1981. doi:10.1177/030098588101800607.

Inglis JT, Macpherson JM. Bilateral labyrinthectomy in the cat: effects on the postural response to translation. *J Neurophysiol* 73: 1181–1191, 1995. doi:10.1152/jn.1995.73.3.1181.

Jankowska E. Interneuronal relay in spinal pathways from proprioceptors. *Prog Neurobiol* 38: 335–378, 1992. doi:10.1016/0301-0082(92)90024-9.

Joseph Jilk D, Safavynia SA, Ting LH. Contribution of vision to postural behaviors during continuous support-surface translations. *Exp Brain Res* 232: 169–180, 2014. doi:10.1007/s00221-013-3729-4.

Kargo WJ, Nitz DA. Early skill learning is expressed through selection and tuning of cortically represented muscle synergies. *J Neurosci* 23: 11255–11269, 2003. doi:10.1523/JNEUROSCI.23-35-11255.2003.

Kutch JJ, Valero-Cuevas FJ. Challenges and new approaches to proving the existence of muscle synergies of neural origin. *PLoS Comput Biol* 8: e1002434, 2012. doi:10.1371/journal.pcbi.1002434.

Laporte Y, Lloyd DP. Nature and significance of the reflex connections established by large afferent fibers of muscular origin. *Am J Physiol* 169: 609–621, 1952. doi:10.1152/ajplegacy.1952.169.3.609.

Lee DD, Seung HS. Learning the parts of objects by non-negative matrix factorization. *Nature* 401: 788–791, 1999. doi:10.1038/44565.

Lemay MA, Grill WM. Modularity of motor output evoked by intraspinal microstimulation in cats. *J Neurophysiol* 91: 502–514, 2004. doi:10.1152/jn.00235.2003.

Levine AJ, Hinckley CA, Hilde KL, Driscoll SP, Poon TH, Montgomery JM, Pfaff SL. Identification of a cellular node for motor control pathways. *Nat Neurosci* 17: 586–593, 2014. doi:10.1038/nn.3675.

Lloyd DP, Chang HT. Afferent fibers in muscle nerves. *J Neurophysiol* 11: 199–207, 1948. doi:10.1152/jn.1948.11.3.199.

Lloyd DP, McIntyre AK. Analysis of forelimb-hindlimb reflex activity in acutely decapitate cats. *J Neurophysiol* 11: 455–470, 1948. doi:10.1152/jn.1948.11.5.455.

Lockhart DB, Ting LH. Optimal sensorimotor transformations for balance. *Nat Neurosci* 10: 1329–1336, 2007. doi:10.1038/nn1986.

Loeb EP, Giszter SF, Borghesani P, Bizzi E. Effects of dorsal root cut on the forces evoked by spinal microstimulation in the spinalized frog. *Somatosens Mot Res* 10: 81–95, 1993. doi:10.3109/08990229309028826.

Lundberg A. Multisensory control of spinal reflex pathways. *Prog Brain Res* 50: 11–28, 1979. doi:10.1016/S0079-6123(08)60803-1.

Macpherson JM. Strategies that simplify the control of quadrupedal stance. II. Electromyographic activity. *J Neurophysiol* 60: 218–231, 1988. doi:10.1152/jn.1988.60.1.218.

Macpherson JM, Everaert DG, Stapley PJ, Ting LH. Bilateral vestibular loss in cats leads to active destabilization of balance during pitch and roll rotations of the support surface. *J Neurophysiol* 97: 4357–4367, 2007. doi:10.1152/jn.01338.2006.

Macpherson JM, Lywood DW, Van Eyken A. A system for the analysis of posture and stance in quadrupeds. *J Neurosci Methods* 20: 73–82, 1987. doi:10.1016/0165-0270(87)90040-9.

Markin SN, Lemay MA, Prilutsky BI, Rybak IA. Motoneuronal and muscle synergies involved in cat hindlimb control during fictive and real locomotion: a comparison study. *J Neurophysiol* 107: 2057–2071, 2012. doi:10.1152/jn.00865.2011.

Nardone A, Tarantola J, Miscio G, Pisano F, Schenone A, Schieppati M. Loss of large-diameter spindle afferent fibres is not detrimental to the control of body sway during upright stance: evidence from neuropathy. *Exp Brain Res* 135: 155–162, 2000. doi:10.1007/s002210000513.

Peterka RJ. Sensorimotor integration in human postural control. *J Neurophysiol* 88: 1097–1118, 2002. doi:10.1152/jn.2002.88.3.1097.

Rao DB, Jortner BS, Sills RC. Animal models of peripheral neuropathy due to environmental toxicants. *ILAR J* 54: 315–323, 2014. doi:10.1093/ilar/ilt058.

Rexed B, Therman PO. Calibre spectra of motor and sensory nerve fibres to flexor and extensor muscles. *J Neurophysiol* 11: 133–139, 1948. doi:10.1152/jn.1948.11.2.133.

Rodriguez KL, Roemmich RT, Cam B, Fregly BJ, Hass CJ. Persons with Parkinson's disease exhibit decreased neuromuscular complexity during gait. *Clin Neurophysiol* 124: 1390–1397, 2013. doi:10.1016/j.clinph.2013.02.006.

Roh J, Cheung VC, Bizzi E. Modules in the brain stem and spinal cord underlying motor behaviors. *J Neurophysiol* 106: 1363–1378, 2011. doi:10.1152/jn.00842.2010.

Routson RL, Clark DJ, Bowden MG, Kautz SA, Neptune RR. The influence of locomotor rehabilitation on module quality and post-stroke hemiparetic walking performance. *Gait Posture* 38: 511–517, 2013. doi:10.1016/j.gaitpost.2013.01.020.

Routson RL, Kautz SA, Neptune RR. Modular organization across changing task demands in healthy and poststroke gait. *Physiol Rep* 2: e12055, 2014. doi:10.14814/phy2.12055.

Saltiel P, Wyler-Duda K, d'Avella A, Ajemian RJ, Bizzi E. Localization and connectivity in spinal interneuronal networks: the adduction-caudal extension-flexion rhythm in the frog. *J Neurophysiol* 94: 2120–2138, 2005. doi:10.1152/jn.00117.2005.

Saltiel P, Wyler-Duda K, D'Avella A, Tresch MC, Bizzi E. Muscle synergies encoded within the spinal cord: evidence from focal intraspinal NMDA iontophoresis in the frog. *J Neurophysiol* 85: 605–619, 2001. doi:10.1152/jn.2001.85.2.605.

Santuz A, Akay T, Mayer WP, Wells TL, Schroll A, Arampatzis A. Modular organization of murine locomotor pattern in the presence and absence of sensory feedback from muscle spindles. *J Physiol* 597: 3147–3165, 2019. doi:10.1113/JP277515.

Sawers A, Allen JL, Ting LH. Long-term training modifies the modular structure and organization of walking balance control. *J Neurophysiol* 114: 3359–3373, 2015b. doi:10.1152/jn.00758.2015.

Schaumburg H, Kaplan J, Windebank A, Vick N, Rasmus S, Pleasure D, Brown MJ. Sensory neuropathy from pyridoxine abuse. A new megavitamin syndrome. *N Engl J Med* 309: 445–448, 1983. doi:10.1056/NEJM198308253090801.

Sohn MH, McKay JL, Ting LH. Defining feasible bounds on muscle activation in a redundant biomechanical task: practical implications of redundancy. *J Biomech* 46: 1363–1368, 2013 [Erratum in *J Biomech* 46: 1976, 2013]. doi:10.1016/j.jbiomech.2013.01.020.

Stapley PJ, Ting LH, Hulliger M, Macpherson JM. Automatic postural responses are delayed by pyridoxine-induced somatosensory loss. *J Neurosci* 22: 5803–5807, 2002. doi:10.1523/JNEUROSCI.22-14-05803.2002.

Stapley PJ, Ting LH, Kuifu C, Everaert DG, Macpherson JM. Bilateral vestibular loss leads to active destabilization of balance during voluntary head turns in the standing cat. *J Neurophysiol* 95: 3783–3797, 2006. doi:10.1152/jn.00034.2006.

Steele KM, Rozumalski A, Schwartz MH. Muscle synergies and complexity of neuromuscular control during gait in cerebral palsy. *Dev Med Child Neurol* 57: 1176–1182, 2015b. doi:10.1111/dmcn.12826.

Steele KM, Tresch MC, Perreault EJ. Consequences of biomechanically constrained tasks in the design and interpretation of synergy analyses. *J Neurophysiol* 113: 2102–2113, 2015a. doi:10.1152/jn.00769.2013.

Stein PS, Daniels-McQueen S. Modular organization of turtle spinal interneurons during normal and deletion fictive rostral scratching. *J Neurosci* 22: 6800–6809, 2002. doi:10.1523/JNEUROSCI.22-15-06800.2002.

Ting LH, Chiel HJ, Trumbower RD, Allen JL, McKay JL, Hackney ME, Kesar TM. Neuromechanical principles underlying movement modularity and their implications for rehabilitation. *Neuron* 86: 38–54, 2015. doi:10.1016/j.neuron.2015.02.042.

Ting LH, Macpherson JM. Ratio of shear to load ground-reaction force may underlie the directional tuning of the automatic postural response to rotation and translation. *J Neurophysiol* 92: 808–823, 2004. doi:10.1152/jn.00773.2003.

Ting LH, Macpherson JM. A limited set of muscle synergies for force control during a postural task. *J Neurophysiol* 93: 609–613, 2005. doi:10.1152/jn.00681.2004.

Torres-Oviedo G, Macpherson JM, Ting LH. Muscle synergy organization is robust across a variety of postural perturbations. *J Neurophysiol* 96: 1530–1546, 2006. doi:10.1152/jn.00810.2005.

Torres-Oviedo G, Ting LH. Muscle synergies characterizing human postural responses. *J Neurophysiol* 98: 2144–2156, 2007. doi:10.1152/jn.01360.2006.

Torres-Oviedo G, Ting LH. Subject-specific muscle synergies in human balance control are consistent across different biomechanical contexts. *J Neurophysiol* 103: 3084–3098, 2010. doi:10.1152/jn.00960.2009.

Turrigiano GG, Nelson SB. Hebb and homeostasis in neuronal plasticity. *Curr Opin Neurobiol* 10: 358–364, 2000. doi:10.1016/S0959-4388(00)00091-X.

Turrigiano GG, Nelson SB. Homeostatic plasticity in the developing nervous system. *Nat Rev Neurosci* 5: 97–107, 2004. doi:10.1038/nrn1327.

Xu Y, Sladky JT, Brown MJ. Dose-dependent expression of neuronopathy after experimental pyridoxine intoxication. *Neurology* 39: 1077–1083, 1989. doi:10.1212/wnl.39.8.1077.

Zar J. *Biostatistical Analysis*. Upper Saddle River, NJ: Prentice-Hall, 1999.